Available online at www.sciencedirect.com
SCIENCE DIRECT®
European Polymer Journal 41 (2005) 2552–2558
EUROPEAN POLYMER JOURNAL
www.elsevier.com/locate/europolj

Fragmentation of poly(amidoamine) dendrimers in matrix-assisted laser desorption

Juhan Subbi [a,*], Reet Aguraiuja [a], Risto Tanner [a], Veiko Allikmaa [b], Margus Lopp [b]

[a] National Institute of Chemical and Biological Physics, Akadeemia tee 23, 12618 Tallinn, Estonia
[b] Tallinn University Technology, Faculty of Science, Ehitajate tee 5, 19086 Tallinn, Estonia

Received 7 April 2005; received in revised form 26 May 2005; accepted 26 May 2005
Available online 14 July 2005

Abstract

Fragmentation of different generations of poly(amidoamine) dendrimers was explored in five common MALDI matrices: 2,5-dihydroxybenzoic acid (DHB), 4-hydroxy-3-methoxycinnamic acid (FER), α-cyano-4-hydroxycinnamic acid (ACH), 2,4,6-trihydroxyacetophenone (THAP), and 3-hydroxypicolinic acid (HPA). Of these, DHB was the softest matrix and ACH produced significant fragment intensity already at MALDI threshold, FER and THAP being in between. HPA was not a convenient matrix for dendrimers and produced a specific fragmentation pattern. Fragmentation analysis was mainly concentrated on generation G1, which contains already all essential structural elements. Dendrimers showed complicated fragmentation behavior with multiple fragmentation channels in our MALDI experiments. The relative intensities of these channels depended selectively on choice of the matrix and showed dissimilar dependence on the laser pulse energy. This was attributed to different fragmentation mechanisms, due to different protonation pathways, occurring in the same MALDI plume. The fragmentation pathways were proposed for all observed fragmentation channels. All fragmentation sites of protonated ions were found to be directly attached to the protonation sites and the fragmentation was surplus charge driven in this sense. No charge remote fragmentation channels were detected. Cationized dendrimers showed higher stability than the protonated ions.

Keywords: PAMAM dendrimers; MALDI-TOF MS; Fragmentation in MALDI; PSD

1. Introduction

Polyamidoamine (PAMAM) dendrimers are synthetic polymers characterized by a branched structure with multiple amide bonds and amine surface and core. Because of its spherical tree-like shape and a number of identical amino groups on the surface, the compounds have unique chemical and physical characteristics, which make them promising candidates for various applications [1–3]. Therefore, characterization of the fine structure of PAMAM dendrimers is an essential task in order to disentangle the spectra of the complex dendrimer conjugates with biomolecules and bioactive compounds. Several analytical techniques, including laser desorption, electrospray ionization [4,5] and MALDI-TOF [6] mass spectroscopy, were used to characterize dendrimers.

* Corresponding author. Tel.: +372 6398312; fax: +372 6398393.
E-mail address: subbi@kbfi.ee (J. Subbi).

0014-3057/$ - see front matter © 2005 Elsevier Ltd. All rights reserved.
doi:10.1016/j.eurpolymj.2005.05.031

However, there are several processes that are involved in the formation of signals in these MS methods. To interpret complex MALDI MS spectra, deeper understanding of the fragmentation processes is needed. In a previous article, we discussed signals in the MALDI TOF MS spectra of PAMAM dendrimers that arouse from the defects of the dendrimer [7]. In the present study, we focus on the fragmentation process itself and on the fragments that form in the course of laser induced desorption during the MALDI mass spectra generation process.

2. Experimental

2.1. Materials

Fragmentation of different generations of PAMAM dendrimers was explored in five common MALDI matrices: 2,5-dihydroxybenzoic acid (DHB), 4-hydroxy-3-methoxycinnamic acid (FER), α-cyano-4-hydroxycinnamic acid (ACH), 2,4,6-trihydroxyacetophenone (THAP), and 3-hydroxypicolinic acid (HPA). All of these were purchased from Aldrich and were used without further purification. Samples of PAMAM dendrimers were prepared and purified preliminarily according to [7,8].

2.2. Chromatographic purification

PAMAM dendrimers were purified additionally in two ways. First, 1.5 g of the Silasorb Diol 10 μm (Chemapol, Prague, Czech Republic) was mixed with 4.5 ml of water. The slurry was poured into a glass column of 200 mm × ∅10 mm with a glass frit bottom, the adsorbent allowed for subsiding in the flow of water 0.5 ml/min, and the final 120 mm high sediment column was covered with a 2 mm layer of glass wool. Aliquots (1–2 ml) of the sample solution (10 mg/ml) were applied to the column, allowed to soak into the adsorbent and the column was eluted with water of 0.5 ml/min. Fractions of 0.5 ml were collected for subsequent MALDI-TOF MS research. Second, HPLC purification was done in a symmetry C18 column. The eluent system was (A) 0.1% trifluoroacetic acid in water and (B) acetonitrile. The linear gradient 0–50% of B in 20 min was used (1 ml/min). Different fractions were collected for subsequent analysis.

2.3. MALDI measurements

All the spectra were taken with an original linear MALDI mass spectrometer (built at the National Institute of Chemical Physics and Biophysics, Estonia) with delayed extraction, equipped with an ETP AF850H electron multiplier for ion detection and a XeF excimer laser on the wavelength of 351 nm for desorption/ionization. This apparatus provided high sensitivity and extended dynamic range for laser intensity dependent measurements. We could analyze spectra with maximum ion intensities varying over three orders of magnitude. In addition, our mass spectrometer could be used as a simple post source decay (PSD) analyzer. The detector had a 5 kV conversion dynode in front of the electron amplifier. In the acceleration region of the conversion dynode, charged fragments, formed in the field free flight region, were accelerated more than the parent ions, arrived earlier due to smaller mass, and formed a shoulder in front of the line. Neutral fragments were not accelerated at all in this region, they came later, and formed a hump behind the line, see hatched areas in Figs. 1 and 3. This analysis was not quantitative, but it gave useful qualitative information of the internal energy of the parent and prompt fragmentation ions.

For mass calibration in different mass ranges, such standard compounds as substance P, insulin b-chain, bovine insulin and horse heart cytochrome *C* were used.

2.4. Sample preparation for MALDI

The dendrimer solution for analysis was prepared by dissolving 1 mg of purified dendrimer syrup in 1 ml water. Additionally, different dilutions of this solution were made. The matrix solution was prepared by dissolving 10 mg of matrix in 1 ml of 1:1 mixture of deionized water and acetonitrile. An analytical sample was prepared by mixing a dendrimer solution (1 μl) with the matrix solution (1 μl) on a stainless steel probe tip,

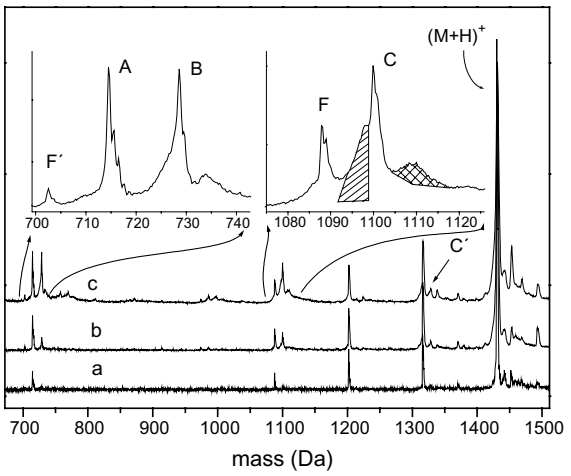

Fig. 1. MALDI mass spectra of G1 with DHB as the matrix, taken with different laser pulse energies: (a) near MALDI threshold energy, (b) about 2× threshold energy, (c) about 3× threshold energy. Capital letters indicate different fragmentation channels, see main text, M designates parent ion. Hatched area shows charged PSD fragments, crosshatched area neutral PSD fragments.

and this mixture was allowed to dry at room temperature. For half generation dendrimers, solutions were made in methanol, to avoid hydrolysis.

3. Results and discussion

Our fragmentation analysis is mainly concentrated on generation G1, which contains all essential structural elements and is in the most convenient mass region for a detailed MS analysis. Also, G1 can be chromatographically purified from higher and lower generations as well as from "structural errors". Additionally, we measured lower and higher generation, as well as half generation dendrimers for comparison. These provided us additional information, especially about single branch fragments that fell into the matrix mass region in the G1 spectra, complicating the interpretation.

3.1. Fragmentation dependence on the laser pulse energy

It was possible to obtain almost unfragmented mass spectra when suitable matrices near MALDI threshold were used. At higher laser intensities, significant fragmentation appeared, and some "hot" matrices produced considerable fragmentation already at the threshold. Furthermore, we observed the existence of several fragmentation channels that showed different dependencies on the choice of the matrix and variation of the laser pulse energy.

The softest matrix tested was the fucose/DHB mixture [7], but for low generations DHB did not produce appreciable fragmentation either. At the threshold, in addition to the main component peak at 1430.02 Da, the mass spectrum of G1 contained only structurally defective dendrimers [7] that were present even after chromatographic purification. However, there appeared one line at exactly half mass of the dendrimer that we attributed to a special fragmentation channel. At higher laser intensities, two more strong fragmentation channels emerged, and at even higher laser intensities, excessive fragmentation stepped in, manifested by many broad bands and higher background, see Fig. 1. The main fragmentation channels of G1 presented in Fig. 1 correspond to the proposed fragmentation sites in Fig. 2. We can distinguish between five principally different fragmentation channels (A, B, C, D and E in Fig. 2). All of these channels assume a transfer of an electron to, or a hydrogen atom from the protonation site, and are surplus charge driven in this sense, see Fig. 3. Fragmentation channels B and C depended strongly on laser intensity, they could be suppressed with soft matrices near the threshold, and at higher laser intensities, they dominated the fragmentation pattern. Channel C′ is an analogue to channel C, only one layer further from the core of the dendrimer, and appeared considerably weaker.

Channel B implies a transfer of an electron from carbon to protonated nitrogen to form a charged alkyl group that probably folds back to nitrogen, forming a

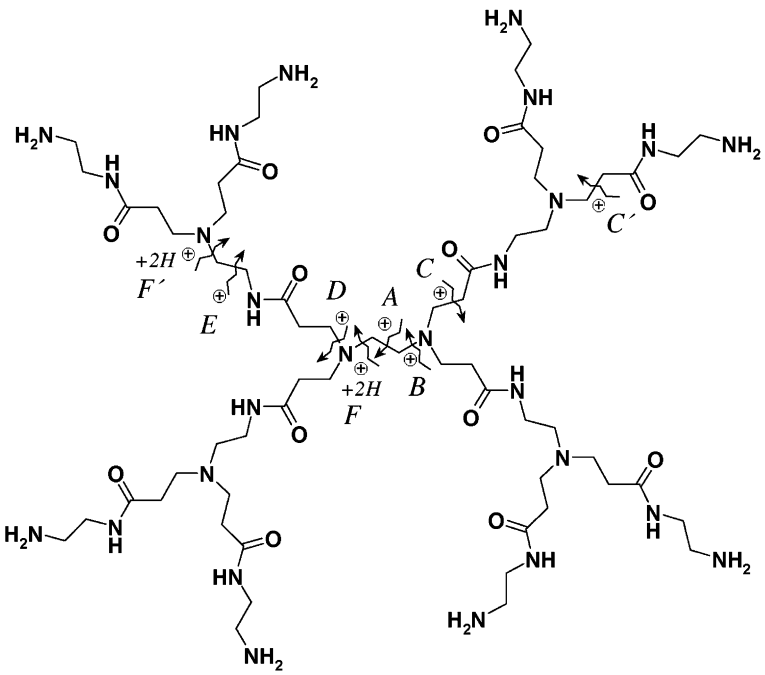

Fig. 2. The first generation PAMAM dendrimer with fragmentation sites, observed in this work. ⊕ indicates the charged fragment.

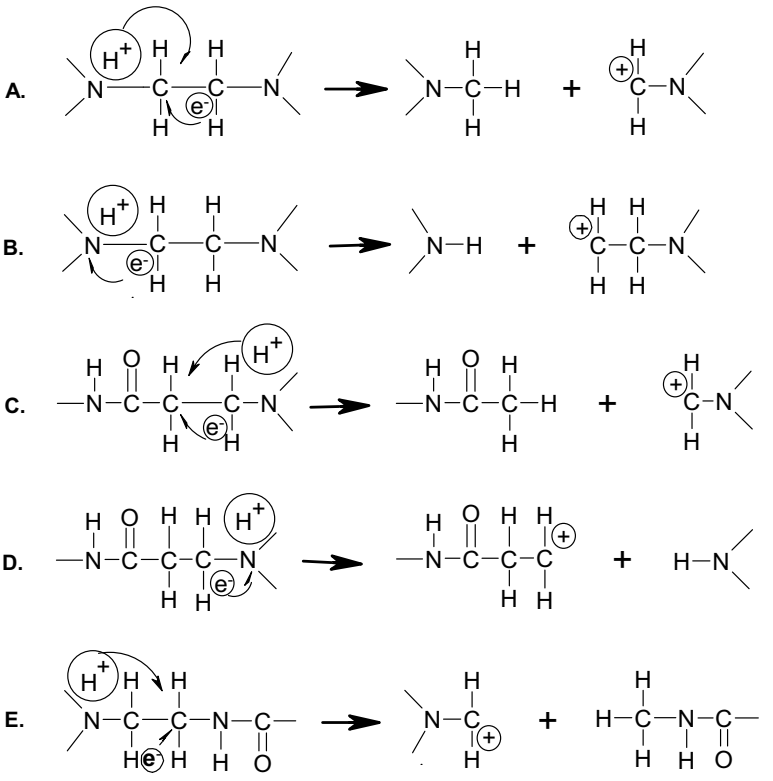

Fig. 3. Proposed mechanisms for observed fragmentation channels.

three membered ring [9]. For channel C fragmentation, the proton from nitrogen, together with an electron (formally a hydrogen atom) has to be transferred to the β-carbon from nitrogen. Comparing gas phase basicities of different amines [10], we found that substituted ethylenediamine core nitrogens are always more basic than other amine nitrogens, making the core nitrogens of the dendrimers preferable protonation sites. This would explain why the fragmentations near the core dominated and channel C′ was weak.

Channel A revealed a different behavior. The charged fragment at exactly half dendrimer mass appeared in all mass spectra, and its abundance depended less on laser intensity than abundance of B and C channel fragments. While near threshold A was the dominating fragmentation channel, at higher laser energies, B and C channel fragments dominated. However, channel A intensity depended strongly on the choice of the matrix.

Fragmentation channels D and E produced charged single branch fragments. These could be observed in the mass region of the matrix induced lines in the spectra of G1 as repeating lines with different matrices, and as dominating lines with high analyte concentrations due to the matrix suppression effect [11,12]. These channels are easily visible in the spectra of higher generation dendrimers, and become the main fragmentation channels in generations 4 and 5 (see Fig. 7). These channels are charge induced like the other three.

These results are in good compliance with both MALDI [9] and electrospray [13] fragmentation analysis of poly(polypropylene imine) dendrimer positive ions. They report analogues to channels B and D as dominant fragmentation pathways. There are three alkyl carbons in every link in these dendrimers instead of two in PAMAM, and no fragmentations between carbons could be detected (these would be analogues to channels A and C).

However, collisional fragmentation of PAMAM dendrimer negative ions gave a completely different pattern, dominated by retro-Michael type reactions [14].

It is interesting to note that we did not observe any fragmentations associated with amide or carbonyl groups. These fragmentation channels dominate in peptides [15] and in synthetic poly(amidoamine) hyperbranched polymers [16], but in PAMAM dendrimers, the amide nitrogens are not basic enough to attract protons, or close enough to protonation sites for a charge induced fragmentation.

There were two more minor fragmentation channels F and F′ forming ions that could be generated from the corresponding defective parent structures as well. However, through different purification routes minimizing

these defects, and comparison to fragmentation patterns of half generation dendrimers, where these defective structures are not possible, we could exclude these fragments from the original sample. For these fragmentations to be energetically feasible in positive ion mode MALDI, in addition to proton transfer, double hydrogen atom transfer is needed, and probably this does not occur in the MALDI plume. We suggest that these fragmentations correspond to retro-Michael reaction that is known to take place in acidic solutions [17], which did happen already in the preparation of the sample or maybe in the solid matrix.

3.2. Fragmentation dependence on the matrix

We obtained the MALDI mass spectra of G1 with all the common matrices listed above. However, from the point of view of fragmentation, the behavior of those matrices was quite different. The softest matrix was the mixture of DHB and fucose 1:1 [7] followed by DHB. Fig. 4 shows the mass spectra of G1 in four other common matrices (THAP, FER, ACH and HPA). The spectra were recorded with laser pulse energy that gave similar intensity for the B and C channel fragmentation. For ACH it was near threshold, for FER and THAP the required energy was considerably higher. With HPA no B and C fragmentations could be obtained, independent of laser pulse energy.

B and C channel fragmentation follows well the accepted hierarchy of "cold" and "hot" matrices: near the threshold, DHB and FER produced almost no fragmentation in these channels, while with ACH the fragmentation into these channels was always visible, and the useful laser pulse energy range was much narrower for ACH. The behavior of THAP was somewhere in between.

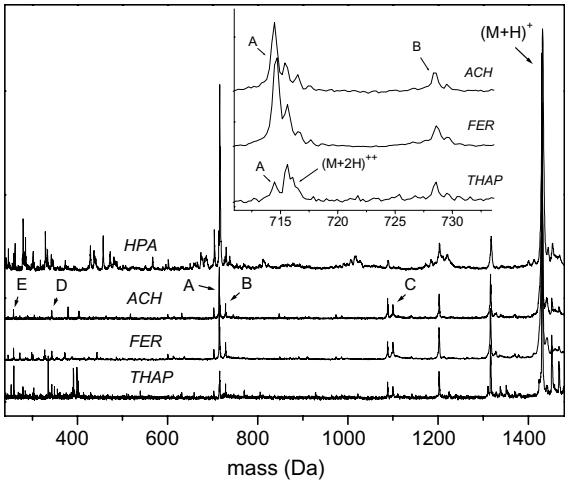

Fig. 4. MALDI mass spectra of G1 with different matrices. Capital letters indicate different fragmentation channels, M designates parent ion.

A well-known cold matrix HPA [18] was a special case. This matrix is widely used for oligonucleotides [19], but it is not a convenient matrix for dendrimers similar for peptides. We were unable to get high resolution and low noise spectra of dendrimers using this matrix. The spectrum appeared only at high laser intensities, and then contained unidentified humps, and lines were wider than with other matrices. However, even at the highest laser intensities, no B or C channel fragmentation was detected. On the other hand, channel A signal was stronger than in the case of any other matrix, and its intensity ratio to the parent ion was practically independent of laser intensity.

Although THAP is not an acidic matrix, it still produced a strong protonated signal. In fact, it was the only matrix that produced a measurable double protonated signal (see Fig. 4) that is remarkable for such a small molecule. At the same time, this matrix causes very little channel A fragmentation, the corresponding line was always smaller than line corresponding to channel B. On the other hand, ACH and FER gave dominant A channel fragmentation at all laser pulse energies, despite one being a hot and the other a cold matrix.

Both protonated and cationized dendrimer ions could be obtained in all matrices, their ratio depending on sample preparation procedures and laser spot localization on the sample, on analogy to peptides containing basic residues. However, fragmentation behavior of protonated and cationized ions was completely different. While protonated ions fragmented strongly at higher laser intensities, cationized ions showed almost no fragmentation (see Fig. 5). The lower fragmentation intensity could be seen in both: lack of cationized fragment ions, and in high stability of cationized parent ions. The PSD shoulders, heavily present in protonated parent and fragment ion lines, are very weak or missing in cationized parent ion lines. Only the channel A fragment at half parent mass had a small cationized companion.

3.3. Post source decay

Broadening of the original mass lines and those corresponding to the fragmentation channels mentioned deserves further attention. The charged fragments that were formed within the time interval between the laser pulse and the ion extraction pulse (530 ns in these experiments) were accelerated like parent ions, and they formed sharp lines in the mass spectrum. This process is called "prompt fragmentation" in the context of the present work. However, shoulders in front of the lines and humps behind them (see Figs. 1 and 5) witness the fragmentation occurring during the flight between the ion source and the ion detector entrance. This fragmentation happens due to the internal energy of the ions and

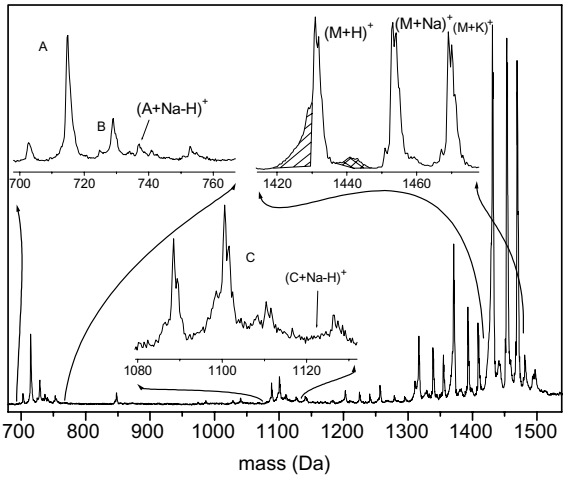

Fig. 5. MALDI mass spectrum of G1 in ACH matrix with both protonated and cationized ions present. Visible are different PSD properties of protonated and cationized ions and suppression of cationization of fragments. Hatched area shows charged PSD fragments, crosshatched area neutral PSD fragments.

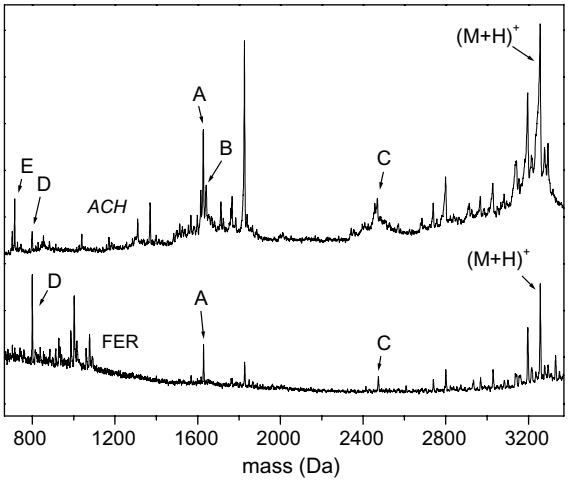

Fig. 6. MALDI mass spectra of G2 with different matrices. Visible are different intensities of fragmentation channels in ACH and FER.

depends on the stability of a particular structure, and on the processes through which ions were formed and conditioned. More fragmentation means more internal energy or lower stability of the ion. We can conclude that cationized dendrimer ions are more stable than the protonated ones, similar to peptides [15]. The B and C fragments are prone to further fragmentation, different from A channel fragments. A more detailed study of the PSD of protonated and cationized dendrimers will be published separately.

3.4. Other generations

A detailed analysis of fragmentation channels is possible for generations up to G3 (see Fig. 6 for G2). The fragmentation channels observed were similar in all generations. However, there appeared also small differences. For example, in G2 channel B was weak and the line corresponding to channel C was wide due to strong PSD. At higher laser intensities, the spectra reveal strong background and low parent ion intensities, manifesting of extensive fragmentation via many overlapping channels. Channels D and E, producing single charged dendrimer branches (that were buried into matrix background in G1), were easily detected in G2. Intensities of these channels are again matrix dependent, channel D being the strongest in ferulic acid, and channel E gaining prominence at higher laser intensities. The fragmentation observed in G1.5 and G2.5 was similar to full generations. In higher generations, the fragmentation channels associated with protonation of core nitrogens were getting less prominent, probably due to many more amine nitrogens available, and dendrimer outer layers hampering the access of the proton donors to the core. On the other hand, fragmentation channels analogous to D and E appeared in the outer dendrimer layers, producing the same fragments as in the case of lower generations.

For generations 4 and 5, a detailed fragmentation analysis was not possible due to low resolution, but we can follow the fragmentation pattern in the lower mass region, the prominent fragment masses corresponding to a single branch (1/4 M) and the second layer single branch (1/8 M) mass regions (see Fig. 7 for G4.5). DHB/fucose matrix produced the least fragmentation, but caused a shift of the mass distribution in the parent ion range to higher masses. This is a general observation for generations 4 and 5, probably due to fucose adducts inside the dendrimer shell that cannot escape in the time scale of the MALDI experiment. Fragmentation in the case of FER produced a significant fragmentation into single branch charged fragments already at MALDI threshold (compare to channel D, G2 in Fig. 6). However, the extent of fragmentation is overestimated here due to the higher sensitivity of the ion detector to lower mass ions. The extent of fragmentation depends on the analyte concentration. Lower concentrations produced less fragmentation, e.g. for G4 to G5 analyte-matrix weight ratio 1:20 was still too high. For smaller analytes, higher concentrations were tolerated, e.g. for G1 the analyte-matrix weight ratio, from which an enhanced fragmentation appeared, was around 1:5. We must keep in mind, however, that for the dried droplet preparation method used in this work, analyte concentration is not well defined.

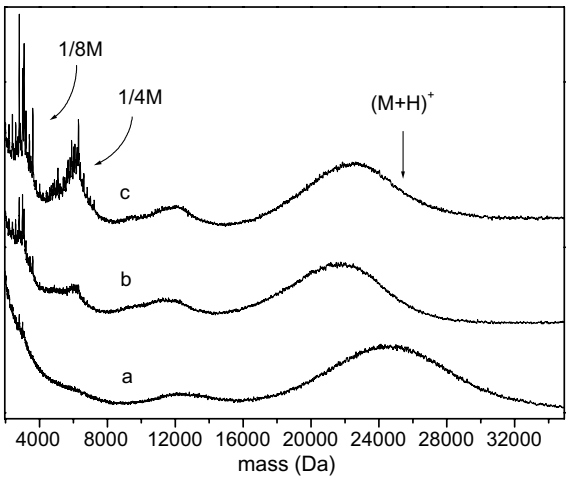

Fig. 7. MALDI mass spectra of G4.5 with mixture of DHB and fucose, matrix to analyte weight ratio 200:1 (a); with FER, matrix to analyte weight ratio 200:1 (b); and with FER, matrix to analyte weight ratio 20:1 (c). Visible are enhanced single branch fragmentations in 1/4 and 1/8 parent mass range in FER, especially at higher concentrations.

3.5. Conclusions

PAMAM dendrimers showed a complicated fragmentation behavior in the MALDI experiments, with multiple fragmentation channels that depend on the matrices and on the laser pulse energy. All fragmentation sites of protonated ions were found to be directly attached to the protonation sites and the fragmentation is surplus charge driven in this sense. No charge remote fragmentation channels were detected.

Cationized dendrimers showed higher stability than the protonated ions we could not detect any fragmentation channels for cationized ions under the conditions where the protonated parent ion signal was comparable to the cationized parent ion signal. Different fragmentation mechanisms, probably due to different protonation pathways, were found to occur in the same MALDI plume, emphasizing the need for detailed studies of the MALDI mechanism in order to interpret all the features of the obtained spectra.

References

[1] Zeng F, Zimmerman SC. Dendrimers in supramolecular chemistry: from molecular recognition to self-assembly. Chem Rev 1997;97:1681–712.
[2] Ardoin N, Astruc D. Molecular trees: from synthesis towards application. Bull Soc Chim Fr 1995;132:875–909.
[3] Kukowska-Latallo JF, Bielinska AU, Johnson J, Spindler R, Tomalia DA, Baker JR. Efficient transfer of genetic material into mammalian cells using starburst polyamidoamine dendrimers. Proc Natl Acad Sci USA 1996;93:4897–902.
[4] Kallos GJ, Tomalia DA, Hedstrand DM, Lewis S, Zhou J. Molecular weight determination of a polyamidoamine starburst polymer by electrospray ionization mass spectromerty. Rapid Commun Mass Spectrom 1991;5:383–6.
[5] Schwartz BL, Rocwood AL, Smith RD, Tomalia DA, Spindler R. Detection of high molecular weight starburst dendrimers by electrospray ionization mass spectrometry. Rapid Comm Mass Spectrom 1995;9:1552–5.
[6] Zhou L, Russell DH, Zhao M, Crooks RM. Characterization of (polyamido)amine dendrimers and their complexes with Cu^{2+} by matrix-assisted laser desorption ionization mass spectrometry. Macromolecules 2001;34: 3567–73.
[7] Peterson J, Allikmaa V, Subbi J, Pehk T, Lopp M. Structure deviations in poly(amidoamine) dendrimers: a MALDI-TOF MS analysis. Eur Polym J 2003;39:33–42.
[8] Peterson J, Ebber A, Allikmaa V, Lopp M. Synthesis and CZE analysis of PAMAM dendrimers with ethylenediamine core. Proc Estonian Acad Sci Chem 2001;50(3):156–66.
[9] Adhiya A, Wesdemiotis C. Poly(propylene imine) dendrimer conformations in the gas phase: a tandem mass spectrometry study. Int J Mass Spectrom 2002;214:75–88.
[10] Hunter EP, Lias SG. In: Mallard WG, Linstrom PJ, editors. NIRT Standard Reference Database Number 69. Gaithersburg, MD: National Institute of Standards and Technology; 1997.
[11] Chan T-WD, Colburn AW, Derrick PJ. Matrix-assisted ultraviolet laser desorption: suppression of the matrix peaks. Org Mass Spectrom 1991;26:342.
[12] Knochenmuss R, Dubois F, Dale MJ, Zenobi R. The matrix suppression effect and ionization mechanisms in matrix-assisted laser desorption/ionization. Rapid Commun Mass Spectrom 1996;10:871–7.
[13] McLuckey SA, Asano KG, Schaaff TG, Stephenson Jr JL. Ion trap collisional activation of protonated poly(propylene imine) dendrimers: generations 1–5. Int J Mass Spectrom 2000;195/196:419–37.
[14] He M, McLuckey SA. Tandem mass spectrometry of half-generation PAMAM dendrimer anions. Rapid Commun Mass Spectrom 2004;18:960–72.
[15] Brown RS, Carr BL, Lennon JJ. Factors that influence the observed fast fragmentation of peptides in matrix-assisted laser desorption. J Am Soc Mass Spectrom 1966;7:225–32.
[16] Hobson LJ, Feast WJ. Poly(amidoamine) hyperbranched systems: synthesis, structure and characterization. Polymer 1999;40:1279–97.
[17] Peterson J, Allikmaa V, Pehk T, Lopp M. Fragmentation of PAMAM dendrimers in methanol. Proc Estonian Acad Sci Chem 2001;50:167–72.
[18] Karas M, Bahr U, Hillenkamp F, Tsarbopolus A, Pramnik BN. Matrix dependence of metastable fragmentation of glycoproteins in MALDI TOF mass spectrometry. Anal Chem 1995;67:675–9.
[19] Chou C, Williams P, Limbach PA. Matrix influence on the formation of positively charged oligonucleotides in matrix-assisted laser desorption/ionization mass spectrometry. Int J Mass Spectrom 1999;193:15–27.